MICROBIAL GENOMICS

RESEARCH ARTICLE

Ko and Choi, *Microbial Genomics* 2021;7:000572

DOI 10.1099/mgen.0.000572

MICROBIOLOGY SOCIETY

OPEN DATA OPEN ACCESS

Comparative genomics reveals an SNP potentially leading to phenotypic diversity of *Salmonella enterica* serovar Enteritidis

Duhyun Ko and Sang Ho Choi*

Abstract

An SNP is a spontaneous genetic change having a potential to modify the functions of the original genes and to lead to phenotypic diversity of bacteria in nature. In this study, a phylogenetic analysis of *Salmonella enterica* serovar Enteritidis, a major food-borne pathogen, showed that eight strains of *S*. Enteritidis isolated in South Korea, including FORC_075 and FORC_078, have almost identical genome sequences. Interestingly, however, the abilities of FORC_075 to form biofilms and red, dry and rough (RDAR) colonies were significantly impaired, resulting in phenotypic differences among the eight strains. Comparative genomic analyses revealed that one of the non-synonymous SNPs unique to FORC_075 has occurred in *envZ*, which encodes a sensor kinase of the EnvZ/OmpR two-component system. The SNP in *envZ* leads to an amino acid change from Pro248 (CCG) in other strains including FORC_078 to Leu248 (CTG) in FORC_075. Allelic exchange of *envZ* between FORC_075 and FORC_078 identified that the SNP in *envZ* is responsible for the impaired biofilm- and RDAR colony-forming abilities of *S*. Enteritidis. Biochemical analyses demonstrated that the SNP in *envZ* significantly increases the phosphorylated status of OmpR in *S*. Enteritidis and alters the expression of the OmpR regulon. Phenotypic analyses further identified that the SNP in *envZ* decreases motility of *S*. Enteritidis but increases its adhesion and invasion to both human epithelial cells and murine macrophage cells. In addition to an enhancement of infectivity to the host cells, survival under acid stress was also elevated by the SNP in *envZ*. Together, these results suggest that the natural occurrence of the SNP in *envZ* could contribute to phenotypic diversity of *S*. Enteritidis, possibly improving its fitness and pathogenesis.

DATA SUMMARY

The whole genome sequences used in this study have been deposited previously in the National Center for Biotechnology Information RefSeq database (https://www.ncbi.nlm.nih.gov/), and the accession numbers are listed in Table S3. The authors confirm that all supporting data and protocols have been provided within the article and through the supplementary data files.

INTRODUCTION

Bacterial pathogens have evolved genetically to adapt to various environmental conditions [1]. Many studies have revealed that genetic mutations occur naturally in bacteria for their optimal fitness and successful pathogenesis during the course of infection [2, 3]. Horizontal gene transfer, one of the possible mechanisms for genetic evolution, results in the acquisition of novel genes and enables non-pathogenic bacteria to be pathogenic [4]. Alternatively, small genetic changes such as SNPs have potential to modify the function of original genes and to induce phenotypic diversity of pathogens, leading to their pathoadaptive evolution [5]. Along with the rapid development of next-generation sequencing technologies, comparative genomic analysis has discovered a number of SNPs occurring in many pathogenic bacteria including *Clostridium difficile*, *Mycobacterium tuberculosis* and *Salmonella enterica* [6–8]. However, studies on the association of each SNP with bacterial pathogenesis are still limited.

Received 05 January 2021; Accepted 29 March 2021; Published 05 May 2021

Author affiliations: [1]National Research Laboratory of Molecular Microbiology and Toxicology, Department of Agricultural Biotechnology and Center for Food and Bioconvergence, Seoul National University, Seoul, Republic of Korea.

***Correspondence:** Sang Ho Choi, choish@snu.ac.kr

Keywords: SNP; pathogenic *Salmonella*; comparative genomics; phenotypic diversity.

Abbreviations: ANI, average nucleotide identity; GAS, group A *Streptococcus*; qRT-PCR, quantitative reverse transcription-PCR; RDAR, red, dry and rough; SAW, smooth and white; SNP, single nucleotide polymorphism; SPI, *Salmonella* pathogenicity island.

Data statement: All supporting data, code and protocols have been provided within the article or through supplementary data files. Five supplementary tables and five supplementary figures are available with the online version of this article.

S. enterica serovar Enteritidis is a major food-borne pathogen, which causes diseases ranging from mild gastroenteritis to severe systemic infection [9, 10]. *Salmonella* has multiple two-component systems to recognize diverse environmental changes and to respond appropriately [11]. The EnvZ/OmpR two-component system has been well studied in *Salmonella*. The sensor kinase EnvZ phosphorylates itself and transfers the phosphoryl group to its cognate response regulator OmpR in response to specific environmental signals such as osmolarity and pH change [12–14]. Phosphorylation induces conformational changes of OmpR, which enhances its DNA binding affinity [15], and thus the expression of the OmpR regulon is mostly dependent on the amount of phosphorylated OmpR (OmpR-P). The OmpR regulon includes *ompF* and *ompC*, which encode outer membrane porins, and regulation of their expression is well characterized. A low level of OmpR-P is enough to activate the transcription of *ompF*, but not of *ompC* [16]. In contrast, a high level of OmpR-P activates *ompC* transcription, while repressing *ompF* transcription [16].

The EnvZ/OmpR two-component system also regulates virulence-related genes and plays an essential role in the pathogenesis of *Salmonella* [17, 18]. For example, the EnvZ/OmpR system controls the expression of *csgD*, which encodes a master regulator activating the biosynthesis of curli fimbriae and cellulose [19–21]. Curli fimbriae and cellulose are major biofilm components and contribute to the development of a red, dry and rough (RDAR) colony morphology [22–24]. In addition, the EnvZ/OmpR system represses expression of flagellar genes such as *fljB* and *fliC*, which are associated with the motility of *Salmonella* [25]. The EnvZ/OmpR system positively regulates the expression of *hilA*, encoding a major activator of virulence genes located in the *Salmonella* pathogenicity island 1 (SPI-1), and the expression of *ssrA* and *ssrB*, encoding a master activator of the SPI-2 genes [26–28]. The SPI-1 and SPI-2 encode type III secretion systems and enable the efficient invasion to host cells and intracellular replication [29–32]. Furthermore, OmpR itself is an acid shock protein and regulates the expression of genes that are necessary for acid resistance [14, 33–35].

In the present study, we conducted a phylogenetic analysis of 241 strains of *S.* Enteritidis and revealed that eight strains isolated in South Korea, including FORC_075 and FORC_078, have almost identical genome sequences. Interestingly, however, distinct phenotypes were observed in FORC_075 which showed an impaired biofilm formation and a smooth and white (SAW) colony morphology. We identified that nine non-synonymous SNPs have occurred exclusively in FORC_075, and one of which is in *envZ* resulting in an amino acid change from Pro248 (C<u>C</u>G) in other strains including FORC_078 to Leu248 (C<u>T</u>G) in FORC_075. By exchanging the SNP allele in *envZ* between FORC_075 and FORC_078, we demonstrate that the SNP in *envZ* determines the biofilm formation and colony morphology. The SNP in *envZ* induces functional modification of EnvZ, increasing the cellular level of OmpR-P in *S.* Enteritidis and altering the expression of the OmpR regulon. Further phenotypic analyses revealed that the SNP in *envZ* decreases motility, but increases both adhesion and invasion to host cells and elevates survival under acid stress. Together, these results suggest that the natural occurrence of the SNP in *envZ* plays a critical role in differentiating the virulence-related phenotypes of *S.* Enteritidis and thus contributes to its phenotypic diversity.

Impact Statement

An SNP is an evolutionary event which contributes to phenotypic diversity of bacteria in nature. Although eight strains of *Salmonella enterica* serovar Enteritidis, a major food-borne pathogen, had almost identical genome sequences, differential phenotypes of biofilm formation and colony morphology were observed among the eight strains. A non-synonymous SNP in *envZ*, encoding a sensor kinase of the EnvZ/OmpR two-component system, was identified to be responsible for the observed differential phenotypes. The SNP in *envZ* affected EnvZ function, increasing the phosphorylated status of OmpR in *S.* Enteritidis and altering the expression of the OmpR regulon. In addition, the SNP in *envZ* significantly differentiated the virulence-related phenotypes of *S.* Enteritidis, including motility, adhesion and invasion to host cells, and even acid resistance. These results suggest that the spontaneous SNP in *envZ* could serve as a pathoadaptive mutation of *S.* Enteritidis, potentially leading to its phenotypic diversity.

METHODS

Strains, plasmids and culture conditions

The strains and plasmids used in this study are listed in Table S1 (available in the online version of this article). Unless otherwise noted, all strains were grown aerobically in Luria-Bertani (LB) medium at 37 °C. When required, antibiotics were added to the medium at the following concentrations: ampicillin, 100 μg ml^{-1}; kanamycin, 100 μg ml^{-1}; and chloramphenicol, 20 μg ml^{-1}. Bacterial growth was monitored spectrophotometrically at 600 nm (A_{600}).

Comparative genomic analyses

The eight whole genome sequences of the *S.* Enteritidis strains, FORC_007, FORC_019, FORC_051, FORC_052, FORC_056, FORC_074, FORC_075 and FORC_078, were retrieved from the NCBI RefSeq database (https://www.ncbi.nlm.nih.gov/). Additionally, the 233 whole genome sequences, which were analysed at 'complete' and 'chromosomal' levels and named as '*Salmonella enterica* subsp. enterica serovar Enteritidis', were retrieved from the NCBI RefSeq database. All accession numbers used in this study are listed in Table S3.

For average nucleotide identity (ANI) analysis, ANI values were calculated by the JSpecies program with the BLAST algorithm comparing 1020 bp fragmented whole genome sequences of the eight FORC strains [36]. For phylogenetic

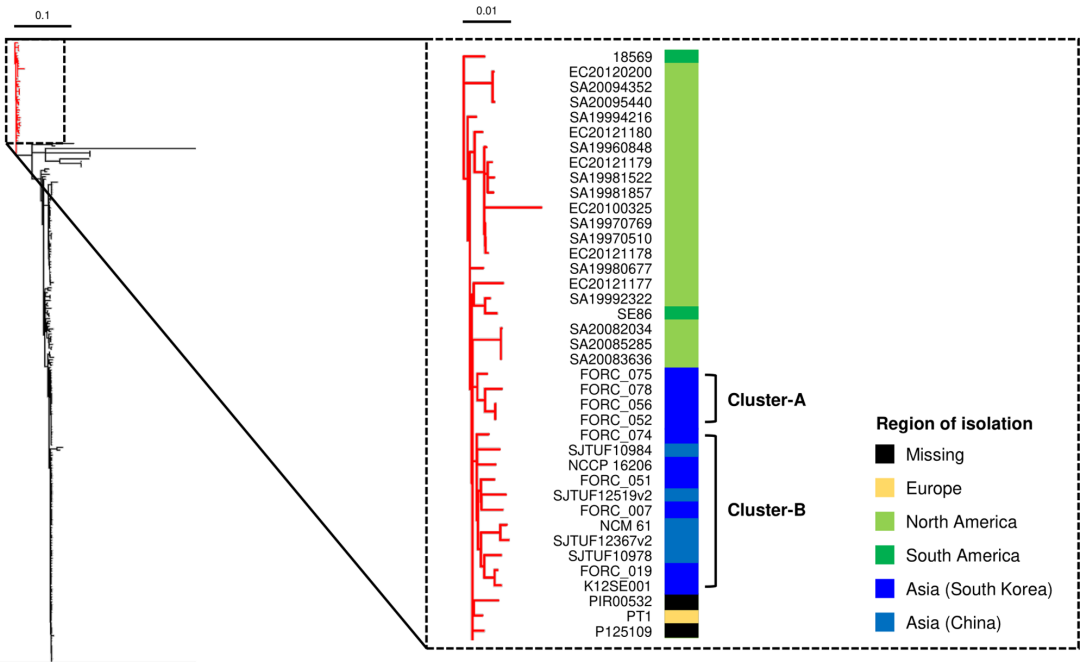

Fig. 1. Phylogenetic tree of the *S.* Enteritidis strains. The phylogenetic relationships were calculated by the RAxML program [39] and visualized using the iTOL program (https://itol.embl.de/) [82]. The branch containing the *S.* Enteritidis strains isolated in South Korea is shown in a dashed box on the right at finer scale. Regions of isolation are indicated in different colour. Bars represent the nucleotide substitutions per site.

analysis, each genome of a total of 241 strains of *S.* Enteritidis was mapped to the genome of *S.* Enteritidis P125109 (reference genome) by the Snippy program (https://github.com/tseemann/snippy). The recombinant region was removed from the resulting alignment by the Gubbins program [37], and then core SNPs were extracted by the SNP-sites program [38]. The extracted SNPs were used to calculate SNP distances between the *S.* Enteritidis strains by the snp-dists program (https://github.com/tseemann/snp-dists). A total of 7154 SNP sites of 241 strains were used to reconstruct a phylogenetic tree by the RAxML program with a gamma distribution and a general time-reversible model under 500 bootstrap repeats [39].

For pangenome analysis, the whole genomes of the eight FORC strains were annotated by the Prokka program [40], and their pangenome was built by the Roary program [41] using the resulting annotations. For SNP analysis, the whole genome sequences of FORC_007, FORC_019, FORC_051, FORC_052, FORC_056, FORC_074 and FORC_075 were aligned to that of FORC_078 by the NUCmer program [42]. SNP positions were inferred by show-snps programs [42], and insertions and deletions were excluded. The effect of non-synonymous SNPs on protein function was predicted by the PROVEAN (Protein variation effect analyzer, http://provean.jcvi.org/) [43], SNAP2 (Screening for non-acceptable polymorphisms 2, https://www.rostlab.org/services/snap/) [44] and SIFT (Sorting intolerant from tolerant, https://sift.bii.a-star.edu.sg/) [45] programs.

Biofilm formation

Biofilms of the *S.* Enteritidis strains were formed as described previously [46] with minor modifications. Briefly, overnight cultures of the *S.* Enteritidis strains were diluted to an A_{600} of 0.01 in tryptic soy broth (1:20 diluted TSB), and 200 µl of the resulting culture was used to form biofilms on each well of 96-well polystyrene microtitre plates (Nunc). After static incubation at 30 °C for 24 or 48 h, the planktonic cells were removed, and the remaining biofilms were stained with 1% crystal violet (CV) solution (Sigma-Aldrich) and quantified as described previously [47].

Colony morphology assay

For analysis of colony morphology, 1 µl of overnight cultures of the *S.* Enteritidis strains was used to spot onto LB agar plates without salt, containing 40 µg ml^{-1} of Congo red (Sigma) and 20 µg ml^{-1} of Coomassie brilliant blue (Sigma) (CR agar plates) or 200 µg ml^{-1} of calcofluor white (Sigma) (CFW agar plates). The resulting colonies were grown at 26 °C for 96 h and visualized using a Stemi 305 stereomicroscope (Zeiss) equipped with an Axiocam 105 colour camera (Zeiss) or photographed using a digital camera (PowerShot G7X Mark II; Canon).

Generation of a *zirT* mutant

The *zirT* gene (FORC78_1136) was inactivated by deletion (1465 bp of 1983 bp) of the coding region using the lambda

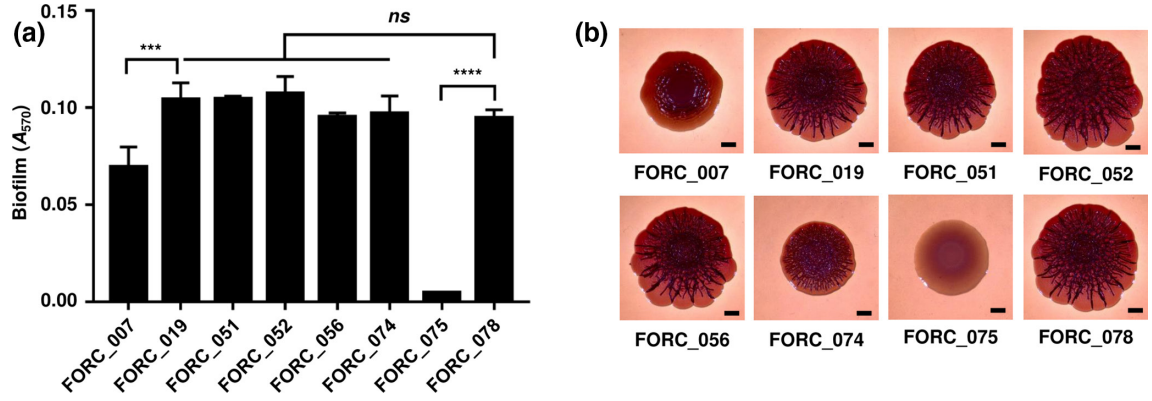

Fig. 2. Distinct biofilm formation and colony morphology of FORC_075. (a) Biofilms of the *S.* Enteritidis strains were grown on 96-well microtitre plates for 48 h and quantified using CV staining. Error bars represent the standard deviation from three independent experiments. Statistical significance was determined by multiple comparisons after one-way ANOVA. ***, $P<0.0005$; ****, $P<0.0001$; *ns*, not significant. (b) The *S.* Enteritidis strains were spotted onto CR agar plates and incubated for 96 h. The colony morphology was visualized using a stereomicroscope (Stemi 305; Zeiss) at 4× magnification. Bars, 2 mm.

red recombination method [48]. Briefly, a linear DNA fragment containing a kanamycin resistance (Km^r) cassette was amplified from pKD13 using ZIRT01-F and ZIRT01-R which were designed to carry 5′- and 3′-flanking regions of *zirT* (Table S2). The resulting fragment was introduced into the *zirT* coding region of FORC_078 carrying pKD46 to generate FORC_078-*zirT*::*kan* (Table S1). The deletion of *zirT* was confirmed by PCR.

Generation of single nucleotide substitution mutants

For single nucleotide substitutions (C → T in *envZ* of FORC_078 and T → C in *envZ* of FORC_075), the *envZ* genes of FORC_078 and FORC_075 were first replaced with a Km^r cassette and chloramphenicol resistance (Cm^r) cassette, respectively, using the lambda red recombination method [48]. Briefly, pairs of primers, ENVZ01-F and ENVZ01-R1 or ENVZ01-F and ENVZ01-R2, which were designed to carry 5′- and 3′-flanking regions of *envZ*, were used for amplification of linear DNA fragments containing the Km^r cassette from pKD13 and the Cm^r cassette from pKD3, respectively (Table S2). The resulting Km^r cassette was introduced into the *envZ* gene of FORC_078 carrying pKD46 to generate FORC_078-*envZ*::*kan*, and the resulting Cm^r cassette was introduced into the *envZ* gene of FORC_075 carrying pKD46 to generate FORC_075-*envZ*::*cat* (Table S1).

Then, the *envZ* region of FORC_078 containing the SNP allele (C) and that of FORC_075 containing the SNP allele (T) were amplified using ENVZ02-F and ENVZ02-R (Table S2), and the resulting fragments were ligated into SphI-SacI-digested pCVD442 to generate pDH1903 and pDH1904, respectively (Table S1). *Escherichia coli* S17-1 λ*pir* containing pDH1903 was used as a conjugal donor to FORC_075-*envZ*::*cat* to generate FORC_075-EnvZ$_{L248P}$ (Table S1). *E. coli* S17-1 λ*pir* containing pDH1904 was used as a conjugal donor to FORC_078-*envZ*::*kan* to generate FORC_078-EnvZ$_{P248L}$ (Table S1). The conjugation and isolation of the transconjugants were conducted using the method described previously [49]. The single nucleotide substitution was confirmed by DNA sequencing. The same experimental procedures were adopted for single nucleotide substitution (C → T) in *envZ* of ATCC 13076 to generate ATCC 13076-EnvZ$_{P248L}$ (Table S1).

Purification of OmpR and Western blot analysis

The *ompR* gene was amplified using OMPR01-F and OMPR01-R (Table S2), and the resulting fragment was subcloned into pET-28a(+) (Novagen) to generate pDH2003 (Table S1). The His$_6$-tagged OmpR was expressed in *E. coli* BL21(DE3) and purified by affinity chromatography (Qiagen). The purified His$_6$-tagged OmpR was used to raise mouse anti-OmpR polyclonal antibody (AbClon).

For Western blot analysis, the *S.* Enteritidis strains grown to an A_{600} of 2.5 were harvested by centrifugation, and the cells were lysed using B-PER Bacterial Protein Extraction Reagent with Enzymes (Thermo Fisher Scientific). The cell debris was removed by centrifugation to obtain clear cell lysates. OmpR and DnaK in the clear cell lysates were detected by Western blot analysis using mouse anti-*S.* Enteritidis OmpR antibody and mouse anti-*E. coli* DnaK antibody (Enzo Life Science) as described previously [50]. The phosphorylated status of OmpR was detected by Western blot analysis using 10% SuperSep Phos-tag precast gels (Wako). After electrophoresis, the precast gels were washed three times with transfer buffer (25 mM Tris, 192 mM glycine, 20% methanol and 5 mM EDTA) to remove Zn^{2+} and further washed once with transfer buffer without EDTA. The phosphorylated- and unphosphorylated-OmpR were detected using the same mouse anti-*S.* Enteritidis OmpR antibody.

Table 1. Non-synonymous SNPs unique to strain FORC_075

Position in FORC_078 (nucleotide)*	Position in FORC_075 (nucleotide)†	Amino acid change	Gene	Function	PROVEAN score (prediction)	SNAP2 score (prediction)	SIFT score (prediction)‡
467447 (G)	1806812 (A)	E113K	*phsA*	Thiosulfate reductase	1.142 (neutral)	−61 (neutral)	1.00 (tolerated)
943379 (C)	2282762 (T)	G186S	–	Peptidase	−5.526 (deleterious)	60 (effect)	N/A
949118 (C)	2288501 (T)	P176L	*bioD*	ATP-dependent dethiobiotin synthetase	−9.206 (deleterious)	59 (effect)	0.00 (affect protein function)
1754770 (A)	3084775 (C)	E142A	*dps*	Non-specific DNA-binding protein Dps	−0.073 (neutral)	−12 (neutral)	0.27 (tolerated)
2115383 (C)	3445390 (T)	A139T	*ybaO*	HTH-type transcriptional regulator YbaO	−3.746 (deleterious)	59 (effect)	0.14 (tolerated)
2331756 (G)	3661765 (A)	P161S	–	Chitinase	−3.649 (deleterious)	33 (effect)	0.01 (affect protein function)
2704053 (A)	4034070 (G)	H109R	*hypT*	HOCl-specific transcription factor HypT	−7.449 (deleterious)	72 (effect)	0.59 (tolerated)
2769014 (G)	4099014 (A)	S510N	*nrdD*	Ribonucleotide reductase of class III (anaerobic), large subunit	1.705 (neutral)	−97 (neutral)	0.59 (tolerated)
3757731 (C)	380056 (T)	P248L	*envZ*	Osmolarity sensory histidine kinase EnvZ	−9.653 (deleterious)	73 (effect)	0.00 (affect protein function)

*The nucleotide position in the chromosome of FORC_078 (RefSeq assembly accession number GCF_004135835.1).
†The nucleotide position in the chromosome of FORC_075 (RefSeq assembly accession number GCF_003429365.1).
‡N/A, not analysed by the server.

RNA purification and transcript analysis

Total RNAs were isolated from the *S*. Enteritidis strains grown to an A_{600} of 2.5 by using an RNeasy mini kit (Qiagen). For quantitative reverse transcription-PCR (qRT-PCR), cDNA was synthesized from 1 µg of the total RNAs by using an iScript cDNA synthesis kit (Bio-Rad). Real-time PCR amplification of the cDNA was performed by using a CFX96 real-time PCR detection system (Bio-Rad) with pairs of specific primers (Table S2) as described previously [51]. Relative expression levels of each gene were calculated by using the 16S rRNA expression level as the internal reference for normalization.

Motility, adhesion, invasion and acid resistance assay

For motility assays, 2 µl of the *S*. Enteritidis strains grown to an A_{600} of 2.5 was used to stab into LB semisolid medium containing 0.3% agar. The plates were incubated at 37 °C for 7 h, and the migration area of cells was visualized by a Gel Doc EZ Imager (Bio-Rad).

For adhesion assays, HeLa human epithelial cells and RAW 264.7 murine macrophage cells were grown in Dulbecco's modified Eagle medium (DMEM) (Gibco-BRL) supplemented with 10% FBS, 100 U ml^{-1} penicillin and 100 µg ml^{-1} streptomycin. One day before bacterial infection, the HeLa cells and RAW 264.7 cells were seeded into 24-well tissue culture plates at a concentration of 2.5×10^5 cells per well and incubated at 37 °C under 5% CO_2. Each well was infected with the *S*. Enteritidis strains grown to an A_{600} of 2.5 at an m.o.i. of 10, centrifuged immediately at 500 ***g*** for 5 min, and then incubated for 30 min. The wells were washed three times with PBS to remove non-adherent bacteria and then lysed in 1% Triton X-100 for 30 min. For invasion assays, the wells were further incubated for 30 min with DMEM supplemented with 100 µg ml^{-1} gentamicin to kill extracellular bacteria before lysis with 1% Triton X-100. The adhered and intracellular bacteria were diluted in PBS and plated on LB agar to enumerate the c.f.u.

For acid resistance assays, the *S*. Enteritidis strains grown to an A_{600} of 2.5 were washed once with PBS (acid-unadapted bacteria) or further incubated in M9 minimal medium containing 10 mM glucose (M9G) (pH 4.3) at 37 °C for 2 h (acid-adapted bacteria). Then, the acid-unadapted and

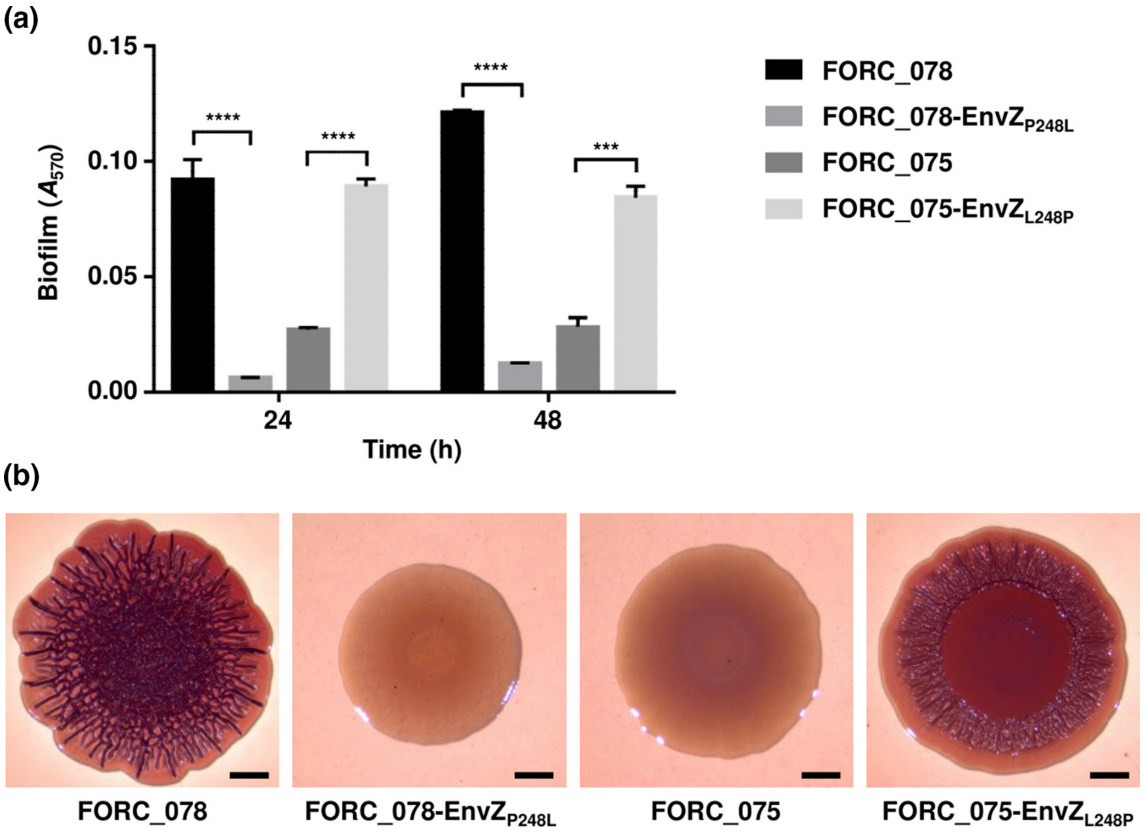

Fig. 3. SNP in *envZ* responsible for the distinct biofilm phenotypes. (a) Biofilms of the *S*. Enteritidis strains were grown on a 96-well microtitre plate for 24 and 48 h and quantified using CV staining. Error bars represent the standard deviation from three independent experiments. Statistical significance was determined by Student's *t*-test. ***, $P<0.0005$; ****, $P<0.0001$. (b) The *S*. Enteritidis strains were spotted onto CR agar plates and incubated for 96 h. Colony morphology was visualized using a stereomicroscope (Stemi 305; Zeiss) at 4× magnification. Bars, 2 mm. FORC_078 and FORC_075, parent strains; FORC_078-$EnvZ_{P248L}$, FORC_078 expressing $EnvZ_{P248L}$; FORC_075-$EnvZ_{L248P}$, FORC_075 expressing $EnvZ_{L248P}$.

acid-adapted bacteria were incubated in M9G (pH 3.0) at 37 °C for 2 h. The pH of M9G was adjusted with HCl. Aliquots of the resulting cultures were diluted in PBS and plated on LB agar to enumerate the c.f.u.

Sequence analysis

The protein ID of FORC_075 EnvZ (WP_080165161.1) was submitted to the NCBI Identical Protein Groups database, and a list of *Salmonella* strains expressing the same FORC_075 EnvZ was retrieved. The isolation information of each strain was retrieved from the NCBI BioSample database, and its serovar was predicted by the SISTR (*Salmonella in silico* typing resource) program [52] using the whole genome sequences. All accession numbers are listed in Table S5.

Statistical analysis

Statistical analyses were performed as indicated in the figure legends using GraphPad Prism 7.0 (GraphPad Software). The significance of differences between experimental groups was accepted at a p value of <0.05.

RESULTS

The *S*. Enteritidis strains isolated in South Korea have a close genetic relationship

Previously, eight strains of *S*. Enteritidis isolated from different sources in South Korea were collected and designated as FORC_007, FORC_019, FORC_051, FORC_052, FORC_056, FORC_074, FORC_075 and FORC_078, and their whole genomes were then completely sequenced and deposited in the NCBI GenBank database under accession numbers GCA_001305235.1, GCA_001705055.1, GCA_002313085.1, GCA_002220345.1, GCA_002313105.1, GCA_003515965.1, GCA_003429365.1 and GCA_004135835.1, respectively. To examine their genetic similarity, ANI values were first calculated. Remarkably, the ANI values between each genome were very high, ranging from 99.98% to 100%, which indicates that the eight FORC strains possess almost identical genome sequences. Then, to determine their evolutionary relationship in the context of the *S*. Enteritidis strains isolated in different countries, an SNP-based phylogenetic analysis was performed. Although all FORC strains were isolated from

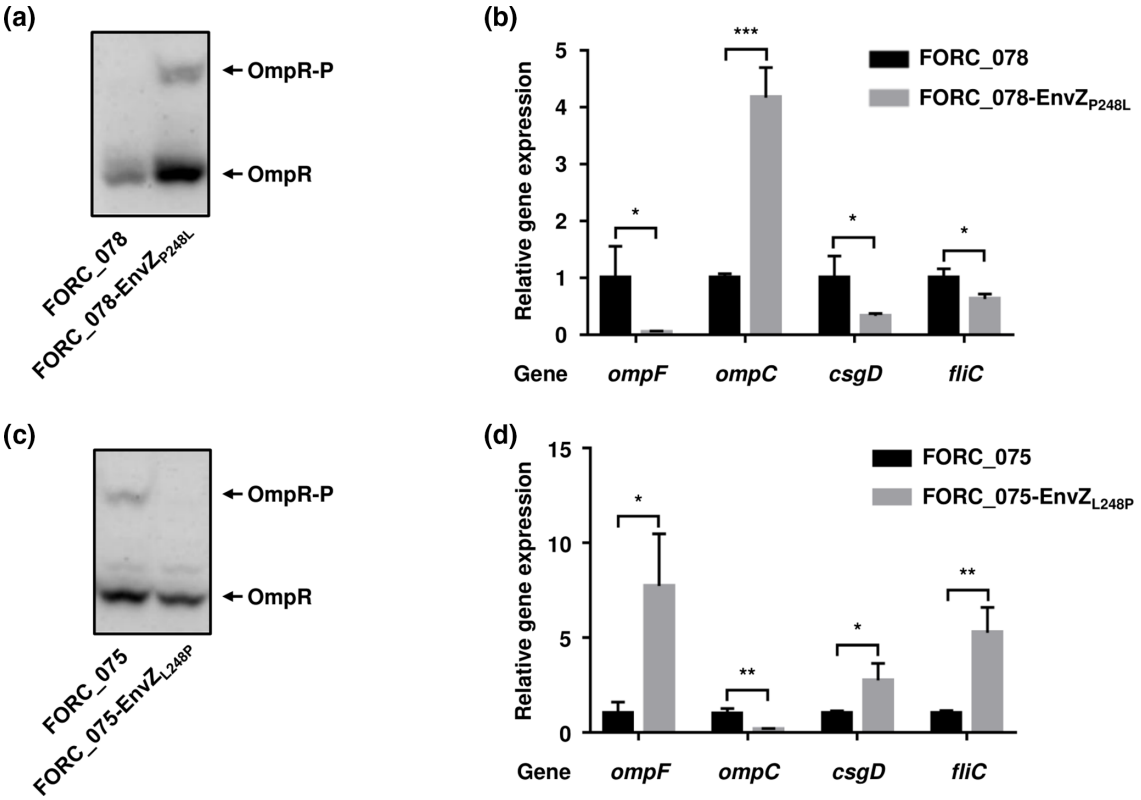

Fig. 4. Effects of the SNP in *envZ* on the OmpR-P level and OmpR regulon expression. Total proteins and RNAs were isolated from the *S.* Enteritidis strains grown to an A_{600} of 2.5. (a, c) The cellular levels of phosphorylated and unphosphorylated OmpR were determined by Western blot analysis using Phos-tag SDS-PAGE gels (Wako). (b, d) Transcript levels of *ompF*, *ompC*, *csgD,* and *fliC* were determined by qRT-PCR. The transcript levels in each parent strain were set as 1. Error bars represent the standard deviation from three independent experiments. Statistical significance was determined by Student's *t*-test. *, $P<0.05$; **, $P<0.005$; ***, $P<0.0005$. FORC_078 and FORC_075, parent strains; FORC_078-$EnvZ_{P248L}$, FORC_078 expressing $EnvZ_{P248L}$; FORC_075-$EnvZ_{L248P}$, FORC_075 expressing $EnvZ_{L248P}$.

different sources or in different years (Table S4), they clustered very closely in the phylogenetic tree (Fig. 1), indicating again that their genetic backgrounds are highly similar. In more detail, the FORC_052, FORC_056, FORC_075 and FORC_078 strains were located in the same branch (Cluster-A in Fig. 1), and the other FORC strains, FORC_007, FORC_019, FORC_051 and FORC_074, clustered together with seven strains isolated in Asia (two from South Korea and five from China) (Cluster-B in Fig. 1). As can be inferred from the phylogenetic tree, the maximum SNP distances within Cluster-A, within Cluster-B, and between the two clusters were 49, 84 and 94, respectively (Fig. S1). The close phylogenetic relationship between the eight FORC strains and the seven Asian strains may result from their relative geographical proximity. Together, these results indicate that the eight FORC strains share their genomic features and have highly similar genetic backgrounds.

FORC_075 exhibits an impaired biofilm formation and a SAW colony morphology

Because the ability of *Salmonella* to form biofilms is important for persistence and survival under environmental stresses [53–56], the biofilm-forming abilities of the eight FORC strains were evaluated. Interestingly, the biofilm-forming ability of FORC_075 was much lower than those of the other FORC strains (Fig. 2a). In particular, the amount of biofilm formed by FORC_075 was approximately 20-fold lower than that formed by FORC_078, a strain phylogenetically closest to FORC_075 (Figs 1 and 2a). One possible hypothesis for the impaired biofilm formation is that FORC_075 has lost the ability to produce the major biofilm components such as curli fimbriae and cellulose. Because both curli fimbriae and cellulose contribute to the development of the RDAR colony morphology [24], the *S.* Enteritidis strains were grown on agar plates containing Congo red (CR agar plates), and their colony morphologies were also compared. FORC_007 formed red and dry colonies with concentric rings (Fig. 2b), which indicates the production of curli fimbriae only [57]. While FORC_019, FORC_051, FORC_052, FORC_056, FORC_074 and FORC_078 formed RDAR colonies, FORC_075 formed SAW colonies, a significantly distinct colony morphology from those of other FORC strains (Fig. 2b). These results support our hypothesis that FORC_075 produces low levels of curli fimbriae and cellulose. To further confirm

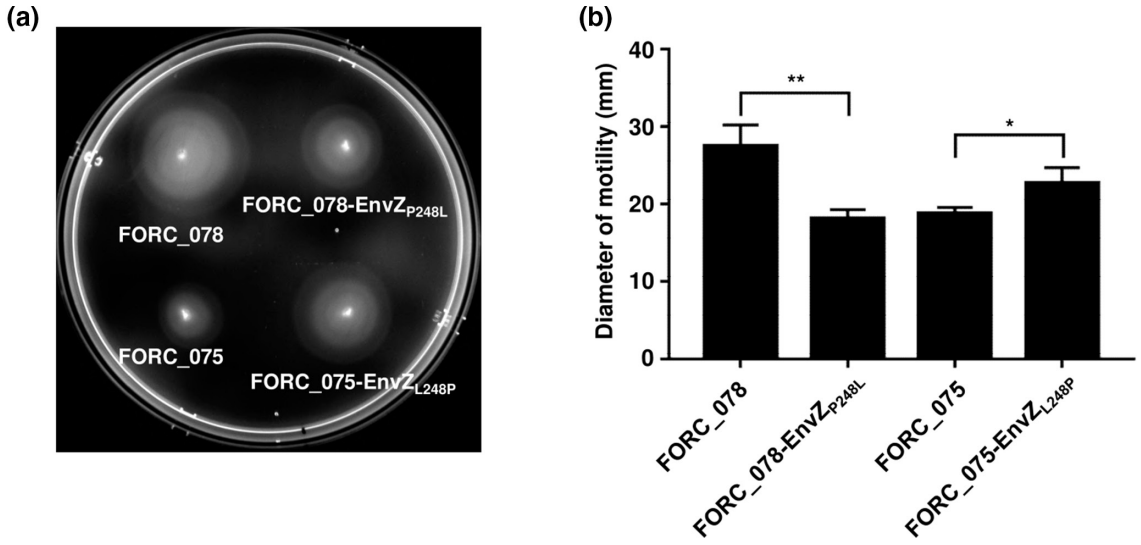

Fig. 5. Effect of SNP in *envZ* on motility. (a) Areas of motility of the *S.* Enteritidis strains grown on LB plates with 0.3% agar for 7 h. (b) Diameter of the areas of motility (mm). Error bars represent the standard deviation from three independent experiments. Statistical significance was determined by Student's *t*-test. *, $P<0.05$; **, $P<0.005$. FORC_078 and FORC_075, parent strains; FORC_078-EnvZ$_{P248L}$, FORC_078 expressing EnvZ$_{P248L}$; FORC_075-EnvZ$_{L248P}$, FORC_075 expressing EnvZ$_{L248P}$.

the cellulose production, the *S.* Enteritidis strains were grown on agar plates containing calcofluor white (CFW agar plates), and their colonies were observed under UV light [23]. Consistent with the results of Fig. 2(b), low fluorescence intensities were observed in the colonies of FORC_007 and FORC_075 compared with those of other FORC strains forming RDAR colonies (Fig. S2), indicating that FORC_007 and FORC_075 produce a small amount of cellulose. Together, these results suggest that the impaired biofilm formation of FORC_075 is due to low levels of both curli fimbriae and cellulose production. Because the genome sequences of the eight FORC strains were almost identical, the significantly different phenotypes of biofilm formation and colony morphology of FORC_075 were unexpected.

A single SNP in *envZ* is responsible for the distinct phenotypes of FORC_075

To elucidate the genetic basis for the unexpected phenotypes of FORC_075, the whole genome sequence of FORC_075 was compared with those of the other FORC strains including FORC_078 using various bioinformatics tools. First, the pangenome of the eight FORC strains was built to identify genes carried differently in the FORC strains. The size of the pangenome was 4767 genes, of which about 91% (4364 genes) constitute the core genome with a length of 4052928 bp, indicating again that the eight FORC strains have similar genetic backgrounds. Among the accessory genome, a total of 10 adjacent genes (FORC78_1133 to FORC78_1142) were not detected just in FORC_075 (Fig. S3a). This region belongs to a genomic island known as GEI 1664/1678 [58], suggesting that genomic rearrangement may have occurred in the FORC_075 genome. In particular, the *zir* operon (FORC78_1134 to FORC78_1137; *zirRTSU*) is conserved throughout the *Salmonella* serovars [59]. The *zirT* gene encodes a membrane transporter ZirT, which mediates secretion of ZirS and ZirU, and this secretion system plays a role as an antivirulence modulator during infection [59, 60]. Because a previous study suggested that the ZirT-dependent secretion system may play a potential role in biofilm formation [60], the *zirT* gene was deleted in the FORC_078 genetic background, and the biofilm- and RDAR colony-forming abilities were determined. However, the biofilm formation and colony morphology of the isogenic *zirT* mutant of FORC_078 were similar to those of the parent strain (Fig. S3b,c). This result indicates that loss of the *zir* operon in the FORC_075 genome is not responsible for its impaired biofilm formation and SAW colony morphology.

Next, the whole genome sequences of the eight FORC strains were compared at the single nucleotide level. Among a total of 198 SNPs detected in the eight strains, nine non-synonymous SNPs were unique to the FORC_075 strain (Table 1). In particular, the two genes containing SNPs, *dps* and *envZ*, are related to biofilm formation [61, 62]. The SNP in *dps* resulted in an amino acid change from Glu142 to Ala142 in Dps, and the SNP in *envZ* resulted in an amino acid change from Pro248 to Leu248 in EnvZ (Table 1). When the effect of each SNP on protein function was predicted *in silico*, the SNP in *dps* was predicted not to have significant effects on the function of Dps (Table 1). In contrast, the SNP in *envZ* was predicted to affect the function of EnvZ (Table 1). Accordingly, the SNP in *envZ* rather than the SNP in *dps* was considered as the most likely candidate responsible for the impaired biofilm formation and SAW colony morphology of FORC_075.

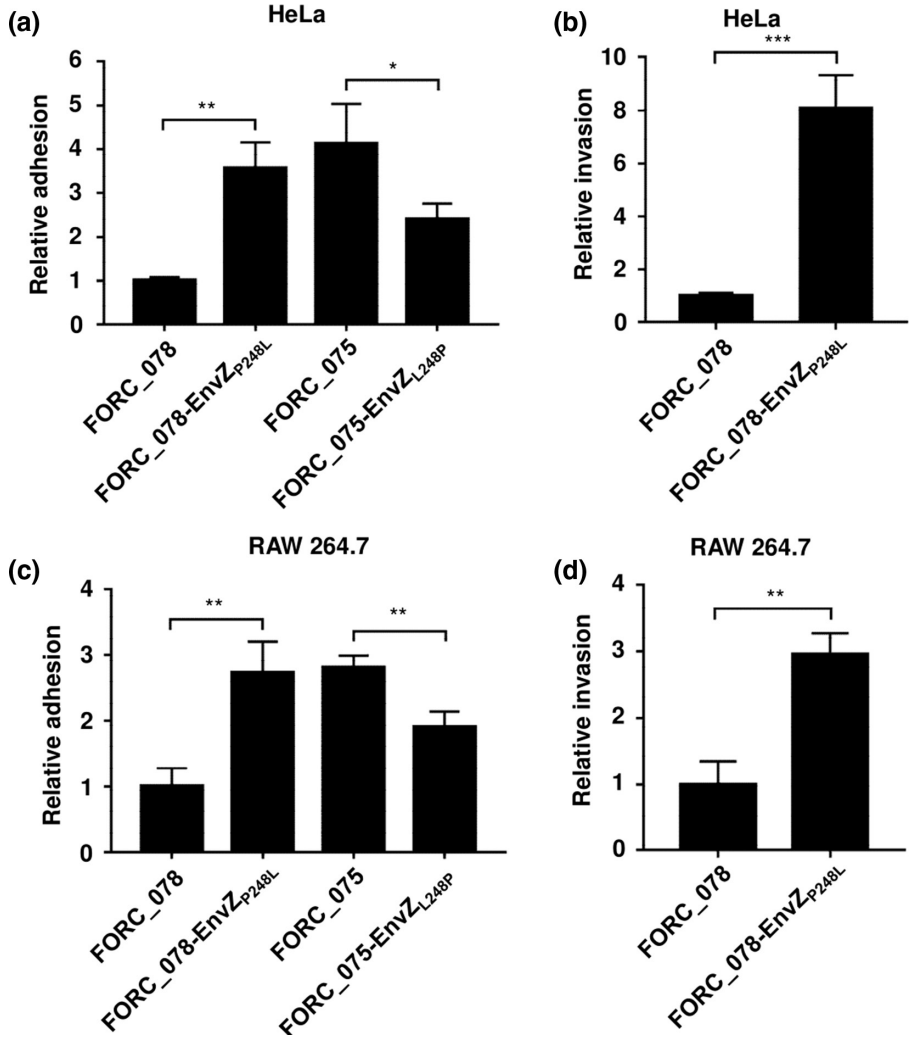

Fig. 6. Effect of SNP in *envZ* on infectivity to host cells. HeLa cells and RAW 264.7 cells were infected with the *S.* Enteritidis strains at an m.o.i. of 10 for 30 min. (a, c) Adhesion to HeLa cells (a) and RAW 264.7 cells (c) expressed as the ratio of the number of adhering cells to the total number of cells used for infection. Relative adhesion of FORC_078 was set as 1. (b, d) Invasion to HeLa cells (b) and RAW 264.7 cells (d) expressed as the ratio of the number of intracellular cells to the total number of cells used for infection. Relative invasion of FORC_078 was set as 1. Error bars represent the standard deviation from three independent experiments. Statistical significance was determined by Student's *t*-test. *, $P<0.05$, **, $P<0.005$, ***, $P<0.0005$. FORC_078 and FORC_075, parent strains; FORC_078-$EnvZ_{P248L}$, FORC_078 expressing $EnvZ_{P248L}$; FORC_075-$EnvZ_{L248P}$, FORC_075 expressing $EnvZ_{L248P}$.

To verify the effects of the SNP in *envZ* on the distinct phenotypes of FORC_075, the SNP alleles of FORC_078 and FORC_075 were exchanged with each other to express $EnvZ_{P248L}$ in FORC_078 and $EnvZ_{L248P}$ in FORC_075, and their biofilm formation and colony morphology were evaluated. The substitution of Pro248 of FORC_078 EnvZ with Leu (P248L) reduced the biofilm-forming ability to the level even lower than that of FORC_075 (Fig. 3a). In addition, the P248L substitution abolished the RDAR colony morphology of FORC_078 and led to the SAW colony morphology similar to that of FORC_075 (Fig. 3b). Although the substitution of Leu248 of FORC_075 EnvZ with Pro (L248P) did not completely restore the ability of FORC_075 to form RDAR colonies to the level comparable to that of FORC_078, the L248P substitution dramatically increased biofilm- and RDAR colony-forming abilities of FORC_075 (Fig. 3). Thus, the combined results indicate that the SNP in *envZ* is a major genetic change determining the ability for biofilm formation and the type of colony morphology of *S.* Enteritidis.

SNP in *envZ* increases OmpR-P level and alters OmpR regulon expression

To determine whether the SNP in *envZ* does indeed affect EnvZ function, the phosphorylated status of OmpR in the *S.* Enteritidis strains was examined. The P248L substitution in the FORC_078 genetic background significantly increased the OmpR-P level (Fig. 4a), while the L248P substitution in the

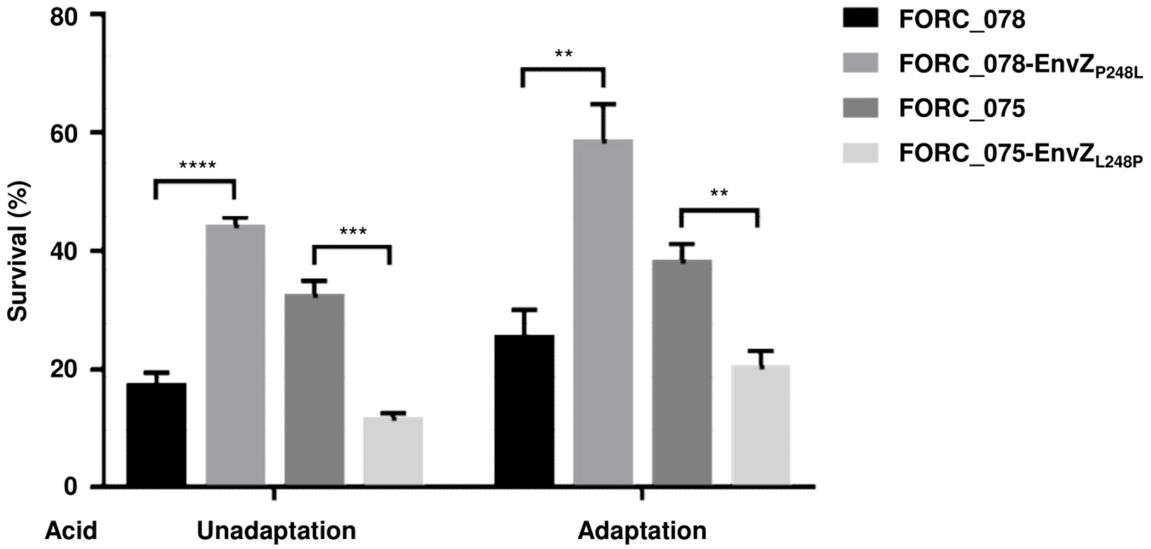

Fig. 7. Effect of the SNP in *envZ* on survival under acid stress. The acid-unadapted and acid-adapted *S.* Enteritidis strains were compared for their abilities to survive under acid stress (pH 3.0). Survival was expressed as the ratio of the number of surviving cells to the number of initially inoculated cells. Error bars represent the standard deviation from three independent experiments. Statistical significance was determined by Student's *t*-test. **, $P<0.005$; ***, $P<0.0005$; ****, $P<0.0001$. FORC_078 and FORC_075, parent strains; FORC_078-$EnvZ_{P248L}$, FORC_078 expressing $EnvZ_{P248L}$; FORC_075-$EnvZ_{L248P}$, FORC_075 expressing $EnvZ_{L248P}$.

FORC_075 genetic background decreased the OmpR-P level to one not detectable by immunoblotting (Fig. 4c). Because the amount of OmpR-P governs *ompF* and *ompC* transcriptions, the effects of the SNP in *envZ* on the expression levels of *ompF* and *ompC* were further investigated. As expected, the P248L substitution resulting in a greater amount of OmpR-P in FORC_078 decreased *ompF* expression by 20-fold and increased *ompC* expression by almost 4-fold (Fig. 4b). Similarly, the L248P substitution resulting in a smaller amount of OmpR-P in FORC_075 increased *ompF* expression and decreased *ompC* expression (Fig. 4d). These results demonstrate that the non-synonymous SNP in *envZ* modifies EnvZ function, increasing the OmpR-P level in *S.* Enteritidis and altering the expression levels of *ompF* and *ompC*.

To examine the effect of the SNP in *envZ* on the expression of the OmpR regulon, expression of *csgD* and *fliC* in the *S.* Enteritidis strains were also compared. Expression of *csgD* in the FORC_078-$EnvZ_{P248L}$ and FORC_075 strains showing increased OmpR-P levels were significantly lower than those in the FORC_078 and FORC_075_{L248P} strains showing decreased OmpR-P levels, respectively (Fig. 4). The results were consistent with previous reports that a high level of OmpR-P has a repressive effect on *csgD* expression [19, 63]. Meanwhile, *fliC* expression was also reduced in the FORC_078 strain by the P248L substitution (Fig. 4b) and elevated in the FORC_075 strain by the L248P substitution (Fig. 4d). To examine the effect of the altered expression of *fliC* on motility, the swimming areas of the *S.* Enteritidis strains on a semisolid plate surface were compared. The diameter of the swimming area of the FORC_078-$EnvZ_{P248L}$ strain was decreased to approximately 70% of that of the FORC_078 strain (Fig. 5). Similar to the decreasing effect of the P248L substitution on motility, the FORC_075 strain was less motile than the FORC_075-$EnvZ_{L248P}$ strain (Fig. 5). This suggests that the SNP in *envZ* decreases the expression level of *fliC* and thus results in reduced motility of *S.* Enteritidis. Collectively, these results indicate that functional modification of EnvZ induced by the SNP in *envZ* increases the phosphorylated status of OmpR and alters the expression of the OmpR regulon, leading to phenotypic changes in biofilm formation and motility of *S.* Enteritidis.

SNP in *envZ* determines the virulence-related phenotypes of *S.* Enteritidis

To extend our understanding of the role of the SNP in *envZ* in *S.* Enteritidis pathogenesis, the effects of the exchange of the SNP allele on the virulence-related phenotypes were examined. When HeLa human epithelial cells and RAW 264.7 murine macrophage cells were infected with the *S.* Enteritidis strains, the adhesion of FORC_078 to the epithelial and macrophage cells was significantly increased by the P248L substitution to the level comparable to that of FORC_075 (Fig. 6a, c). Consistent with this result, the adhesion of FORC_075 to both host cells was reduced by the L248P substitution (Fig. 6a, c). In addition, although it was not possible to assess the invasion of FORC_075 because of its gentamicin resistance (Table S1), the invasion of FORC_078 to HeLa and RAW 264.7 cells was greatly increased by the P248L substitution (Fig. 6b, d). These combined results indicate that the SNP in *envZ* leading to $EnvZ_{L248}$ increases the infectivity of *S.* Enteritidis to host cells.

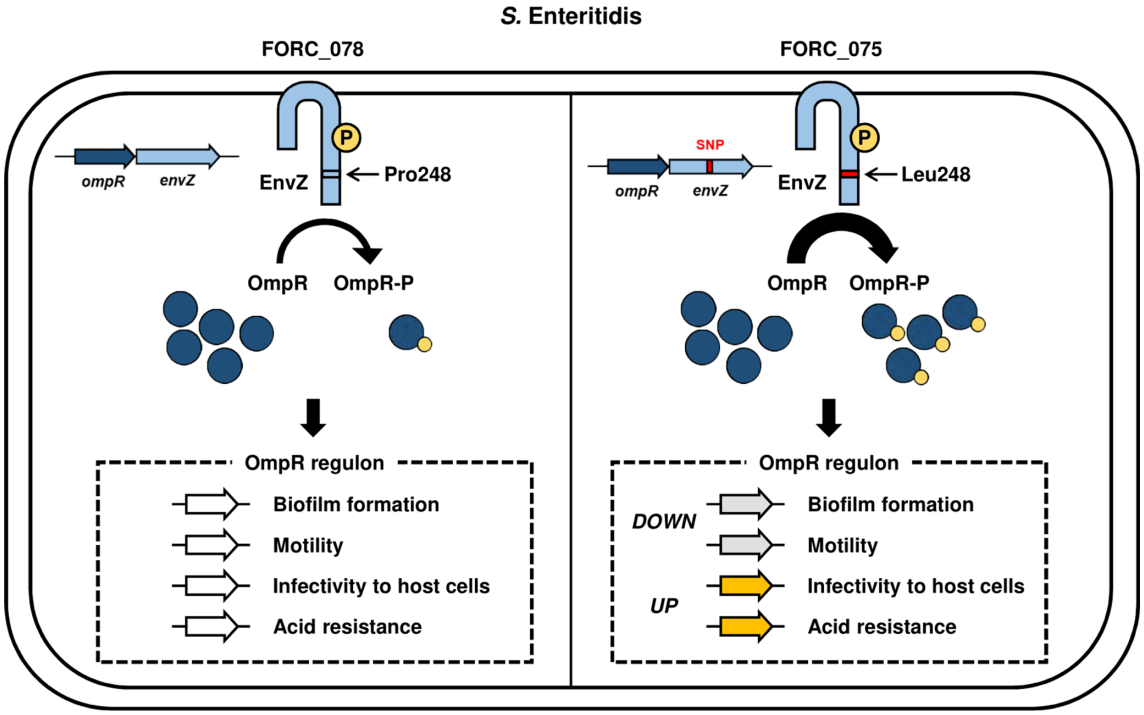

Fig. 8. Proposed model for the effects of the SNP in *envZ*. A non-synonymous SNP in *envZ* of FORC_075 results in amino acid change of EnvZ from Pro248 in FORC_078 to Leu248 in FORC_075. This amino acid change modifies EnvZ function and leads to an increase in the cellular level of OmpR-P. As a result, expression of the OmpR regulon would be altered, which results in the decreases in biofilm formation and motility and the increases in infectivity to host cells and acid resistance. Together, the phenotypic changes induced by the SNP in *envZ* could improve the fitness and pathogenesis of *S.* Enteritidis during infection, increasing the selective pressure on FORC_075.

The effect of the SNP in *envZ* on survival of *S.* Enteritidis under acid stress was also assessed. The survival of acid-unadapted and acid-adapted FORC_078 at pH 3.0 was increased by more than 2-fold by the P248L substitution (Fig. 7). Similarly, the survival of FORC_075 at pH 3.0 was reduced by the L248P substitution to the level comparable to that of FORC_078 in both acid-unadapted and acid-adapted cells (Fig. 7). These results indicate that the SNP in *envZ* leading to $EnvZ_{L248}$ enhances the acid resistance of *S.* Enteritidis, regardless of the previous acid adaptation. Together, the results suggest that the SNP in *envZ* improves *S.* Enteritidis pathogenesis by elevating its infectivity to host cells and survival under acid stress during the course of infection.

Effects of the SNP in *envZ* are not dependent on a particular *S.* Enteritidis genetic background

To investigate whether the effects of the SNP in *envZ* are specific to the FORC strains, an ATCC 13076-$EnvZ_{P248L}$ mutant was constructed using a standard strain of *S.* Enteritidis, ATCC 13076. The P248L substitution in the ATCC 13076 genetic background increased OmpR-P level and altered the expression of the OmpR regulon (Figs S4a, b). Moreover, the P248L substitution decreased biofilm formation of ATCC 13076, while increasing its infectivity to host cells as well as survival under acid stress (Fig. S4c–g). All these results observed in ATCC 13076 were identical to those in FORC_078, suggesting that the effects of the SNP in *envZ* are not dependent on a specific genetic background.

The SNP in *envZ* can naturally occur in other *Salmonella* strains

To determine whether the SNP in *envZ* is also found in other *Salmonella* strains, the presence of the strain expressing $EnvZ_{L248}$, instead of $EnvZ_{P248}$, was examined in the NCBI database. Nine isolates of *Salmonella* including FORC_075 were identified to carry the same SNP in *envZ* (Table S5). The isolation source of BCW_2682 and SLM287 was chicken meat, and that of CFSAN083304 was cattle intestine (Table S5), indicating that the strain expressing $EnvZ_{L248}$ can survive in various environments. These results imply that the spontaneous SNP in *envZ* is not a dead-end mutation.

DISCUSSION

Together with the accumulation of bacterial genomic data, comparative genomic analysis has allowed us to understand dynamic genetic changes leading to phenotypic differences [64, 65]. Acquisition or loss of accessory genes and small genetic changes in core genes may have a significant impact on phenotypes, which increases the virulence and survival of bacterial pathogens under a variety of environmental

stresses. In the present study, we evaluated the phenotypes of eight strains of *S.* Enteritidis whose genetic similarity is very high (Fig. 1). Among the eight strains, however, FORC_075 exhibited distinct phenotypes of biofilm formation and colony morphology (Fig. 2). We demonstrated that an SNP in *envZ* is responsible for the impaired biofilm formation and SAW colony morphology of FORC_075 (Table 1, Fig. 3).

The SNP in *envZ* of FORC_075 resulted in $EnvZ_{L248}$, different from $EnvZ_{P248}$ in other strains including FORC_078 (Table 1). Pro248 is positioned in an H box that is well conserved in sensor kinases including EnvZ and important for its autophosphorylation and phosphotransfer to OmpR [66]. Thus, mutation in Pro248 probably affects the phosphorylated status of OmpR and thereby its activity to regulate downstream genes. In this study, we detected higher OmpR-P levels in the *S.* Enteritidis strains expressing $EnvZ_{L248}$ instead of $EnvZ_{P248}$ (Figs 4a, c and S4a) and also confirmed that expression of the OmpR regulon was significantly altered depending on the amount of OmpR-P (Figs 4b, d and S4b). Interestingly, while the *ompR* mRNA level was not significantly influenced by the SNP in *envZ*, the total OmpR protein level was increased by the SNP in *envZ* (Fig. S5). These results suggest the potential role of Pro248 in the regulation of OmpR expression at the post-transcriptional level, which remains to be studied in the future. Nonetheless, our combined results imply that this SNP has naturally occurred at a critical site in *envZ* that leads to changes in the phosphorylated status of OmpR and in its regulatory activity.

FORC_075 is a clinical strain isolated from human stool (Table S3) and carries the SNP in *envZ* leading to $EnvZ_{L248}$. There are several lines of evidence that genetic changes frequently occur in a sensor kinase of the signal transduction system during host–bacteria interactions, possibly affecting the bacterial pathogenic features. For example, *S.* Typhimurium strains, isolated from gallbladder of mouse, had a truncated mutation in *envZ* and showed hyper-biofilm formation [46]. For group A *Streptococcus* (GAS), signal transduction systems such as the LiaFSR three-component system and CovSR two-component system play an important role in virulence of the pathogen [67, 68]. GAS isolates, recovered from a patient, carried an SNP in the H box of sensor kinase LiaS, and this mutation decreased virulence of a GAS but increased its colonization to host cells [69]. In addition, GAS strains, isolated after mouse infection, contained an amino acid change from Pro285 of sensor kinase CovS (corresponding to Pro248 of EnvZ) to Ser, which affects its phosphatase activity altering the expression of virulence genes [70]. Along with these previous reports, it is possible to suggest that the SNP in *envZ* of the FORC_075 genome also occurred spontaneously during the course of host infection.

During host infection, modulation of the virulence-related phenotypes is important for *S.* Enteritidis to obtain optimal fitness and successful pathogenesis. In this study, we identified that the SNP in *envZ* of FORC_075 decreases biofilm formation and motility but elevates infectivity to host cells and acid resistance (Figs 3 and 5–7). It has been shown that loss of biofilm components could alleviate host immune responses and lead to efficient invasion of *Salmonella* to host cells and its hypervirulence *in vivo* [71–74]. Similarly, flagella are required for motility but stimulate the host immune system, and thus their overexpression results in attenuation of *Salmonella* in the mouse model [75, 76]. Accordingly, the decreased expression of biofilm components and flagella resulting from the SNP in *envZ* is expected to be beneficial for survival of *S.* Enteritidis in host environments by reducing the chances of being detected by the immune system. Furthermore, adhesion and invasion to host cells are essential for *Salmonella* to cause infection, and induction of acid resistance enables the bacteria to survive in acidic conditions such as the stomach [77–79]. Thus, the enhanced infectivity to host cells and acid resistance resulting from the SNP in *envZ* could contribute to *Salmonella* pathogenesis. Together, these phenotypic changes introduced by the SNP in *envZ* may confer selective advantages to the *S.* Enteritidis strains expressing $EnvZ_{L248}$.

In recent years, single nucleotide mutations underlying the clonal expansion of *Salmonella* have been reported, suggesting their evolutionary impact. An SNP in the promoter region of the virulence gene *pgtE*, causing hyperinvasion of *Salmonella*, was proposed as a genetic signature of isolates in *S.* Typhimurium ST313 lineage 2 [80]. In addition, conserved SNPs in multiple loci, leading to impaired biofilm formation of *Salmonella*, were presented as strong evidence of the parallel evolution in invasive *Salmonella* lineages [81]. According to these recent works, we expect that the SNP in *envZ* serves as a pathoadaptive mutation that could potentially play a role in bacterial evolution. The emergence of several *Salmonella* strains carrying the same SNP allele in *envZ* also supports our expectation (Table S5).

In summary, we revealed that eight FORC strains of *S.* Enteritidis had almost identical genome sequences. However, FORC_075 showed impaired biofilm- and RDAR colony-forming abilities, which was distinct from other FORC strains including FORC_078. Among non-synonymous SNPs unique to FORC_075, an SNP in *envZ* leading to an amino acid change from Pro248 to Leu248 was identified to result in the impaired biofilm formation and SAW colony morphology of *S.* Enteritidis. The effects of the SNP in *envZ* on phenotypic changes of *S.* Enteritidis are summarized in Fig. 8. The SNP in *envZ* induced functional modification of EnvZ, which increased the cellular level of OmpR-P in *S.* Enteritidis and altered the expression of the OmpR regulon. The SNP in *envZ* led to the decrease in motility but the increase in adhesion and invasion to host cells and even in acid resistance of *S.* Enteritidis. Together, these results suggest that the SNP in *envZ* plays a key role in differentiating the virulence-related phenotypes. Considering that the EnvZ/OmpR system is highly conserved in *Enterobacteriaceae*, it could be suggested as a good target for development of broad-spectrum antivirulence agents against many pathogens. This study provides insights into the natural occurrence of an SNP that potentially contributes to phenotypic diversity of *S.* Enteritidis for optimal fitness and successful pathogenesis.

Funding information
This research was supported by the National Research Foundation of Korea, funded by the Ministry of Science, ICT, and Future Planning (2017R1E1A1A01074639), and a grant (19162MFDS037) from the Ministry of Food and Drug Safety to S.H.C. The funders had no role in this study.

Author contributions
D.K. and S.H.C. designed the study. D.K. performed experiments and analyses. D.K. and S.H.C. wrote the manuscript.

Conflicts of interest
The authors declare that there are no conflicts of interest.

References

1. Arber W. Genetic variation: molecular mechanisms and impact on microbial evolution. *FEMS Microbiol Rev* 2000;24:1–7.
2. Yang L, Jelsbak L, Marvig RL, Damkiær S, Workman CT *et al*. Evolutionary dynamics of bacteria in a human host environment. *Proc Natl Acad Sci U S A* 2011;108:7481–7486.
3. Lieberman TD, Michel J-B, Aingaran M, Potter-Bynoe G, Roux D *et al*. Parallel bacterial evolution within multiple patients identifies candidate pathogenicity genes. *Nat Genet* 2011;43:1275–1280.
4. Kelly BG, Vespermann A, Bolton DJ. The role of horizontal gene transfer in the evolution of selected foodborne bacterial pathogens. *Food Chem Toxicol* 2009;47:951–968.
5. Sokurenko EV, Hasty DL, Dykhuizen DE. Pathoadaptive mutations: gene loss and variation in bacterial pathogens. *Trends Microbiol* 1999;7:191–195.
6. Collery MM, Kuehne SA, McBride SM, Kelly ML, Monot M *et al*. What's a SNP between friends: The influence of single nucleotide polymorphisms on virulence and phenotypes of *Clostridium difficile* strain 630 and derivatives. *Virulence* 2017;8:767–781.
7. Mikheecheva NE, Zaychikova MV, Melerzanov AV, Danilenko VN. A nonsynonymous SNP catalog of *Mycobacterium tuberculosis* virulence genes and its use for detecting new potentially virulent sublineages. *Gen Biol Evol* 2017;9:887–899.
8. Scaltriti E, Sassera D, Comandatore F, Morganti M, Mandalari C *et al*. Differential single nucleotide polymorphism-based analysis of an outbreak caused by *Salmonella enterica* serovar Manhattan reveals epidemiological details missed by standard pulsed-field gel electrophoresis. *J Clin Microbiol* 2015;53:1227–1238.
9. Chen H-M, Wang Y, Su L-H, Chiu C-H. Nontyphoid Salmonella infection: microbiology, clinical features, and antimicrobial therapy. *Pediatr Neonatol* 2013;54:147–152.
10. European Food Safety Authority and European Centre for Disease Prevention and Control (EFSA and ECDC). The European Union summary report on trends and sources of zoonoses, zoonotic agents and food-borne outbreaks in 2017. *Efsa J* 2018;16:e05500.
11. Capra EJ, Laub MT. Evolution of two-component signal transduction systems. *Annu Rev Microbiol* 2012;66:325–347.
12. Delgado J, Forst S, Harlocker S, Inouye M. Identification of a phosphorylation site and functional analysis of conserved aspartic acid residues of OmpR, a transcriptional activator for *ompF* and *ompC* in *Escherichia coli*. *Mol Microbiol* 1993;10:1037–1047.
13. Wang LC, Morgan LK, Godakumbura P, Kenney LJ, Anand GS. The inner membrane histidine kinase EnvZ senses osmolality via helix-coil transitions in the cytoplasm. *Embo J* 2012;31:2648–2659.
14. Chakraborty S, Winardhi RS, Morgan LK, Yan J, Kenney LJ. Non-canonical activation of OmpR drives acid and osmotic stress responses in single bacterial cells. *Nat Commun* 2017;8:1587.
15. Head CG, Tardy A, Kenney LJ. Relative binding affinities of OmpR and OmpR-phosphate at the *ompF* and *ompC* regulatory sites. *J Mol Biol* 1998;281:857–870.
16. Aiba H, Mizuno T. Phosphorylation of a bacterial activator protein, OmpR, by a protein kinase, EnvZ, stimulates the transcription of the *ompF* and *ompC* genes in *Escherichia coli*. *FEBS Lett* 1990;261:19–22.
17. Dorman CJ, Chatfield S, Higgins CF, Hayward C, Dougan G. Characterization of porin and ompR mutants of a virulent strain of Salmonella typhimurium: ompR mutants are attenuated in vivo. *Infect Immun* 1989;57:2136–2140.
18. Quinn HJ, Cameron ADS, Dorman CJ. Bacterial regulon evolution: distinct responses and roles for the identical OmpR proteins of *Salmonella* typhimurium and *Escherichia coli* in the acid stress response. *PLoS Genet* 2014;10:e1004215.
19. Gerstel U, Park C, Romling U. Complex regulation of *csgD* promoter activity by global regulatory proteins. *Mol Microbiol* 2003;49:639–654.
20. Hammar M, Arnqvist A, Bian Z, Olsen A, Normark S. Expression of two *csg* operons is required for production of fibronectin- and Congo red-binding curli polymers in *Escherichia coli* K-12. *Mol Microbiol* 1995;18:661–670.
21. Romling U, Rohde M, Olsen A, Normark S, AgfD RJ. the checkpoint of multicellular and aggregative behaviour in *Salmonella typhimurium* regulates at least two independent pathways. *Mol Microbiol* 2000;36:10–23.
22. Austin JW, Sanders G, Kay WW, Collinson SK. Thin aggregative fimbriae enhance *Salmonella enteritidis* biofilm formation. *Fems Microbiology Letters* 1998;162:295–301.
23. Solano C, Garcia B, Valle J, Berasain C, Ghigo JM *et al*. Genetic analysis of *Salmonella enteritidis* biofilm formation: critical role of cellulose. *Mol Microbiol* 2002;43:793–808.
24. Römling U. Characterization of the rdar morphotype, a multicellular behaviour in Enterobacteriaceae. *Cell Mol Life Sci* 2005;62:1234–1246.
25. Xu S, Zou X, Sheng X, Zhang H, Mao L *et al*. Expression of *fljB:z66* on a linear plasmid of *Salmonella enterica* serovar Typhi is dependent on fliA and flhDC and regulated by OmpR. *Braz J Microbiol* 2010;41:729–740.
26. Ellermeier CD, Ellermeier JR, Slauch JM. Hild, HilC and RtsA constitute a feed forward loop that controls expression of the SPI1 type three secretion system regulator *hilA* in *Salmonella enterica* serovar typhimurium. *Mol Microbiol* 2005;57:691–705.
27. Feng X, Oropeza R, Kenney LJ. Dual regulation by phospho-OmpR of *ssrA/B* gene expression in Salmonella pathogenicity island 2. *Mol Microbiol* 2003;48:1131–1143.
28. Lee AK, Detweiler CS, Falkow S. OmpR regulates the two-component system SsrA-SsrB in *Salmonella* pathogenicity island 2. *J Bacteriol* 2000;182:771–781.
29. Galán JE. Molecular genetic bases of *Salmonella* entry into host cells. *Mol Microbiol* 1996;20:263–271.
30. Groisman EA, Ochman H. Cognate gene clusters govern invasion of host epithelial-cells by *Salmonella typhimurium* and *Shigella flexneri*. *Embo J* 1993;12:3779–3787.
31. Groisman EA, Ochman H. How *Salmonella* became a pathogen. *Trends Microbiol* 1997;5:343–349.
32. Shea JE, Hensel M, Gleeson C, Holden DW. Identification of a virulence locus encoding a second type III secretion system in *Salmonella typhimurium*. *Proc Natl Acad Sci U S A* 1996;93:2593–2597.
33. Bang IS, Kim BH, Foster JW, Park YK. OmpR regulates the stationary-phase acid tolerance response of *Salmonella enterica* serovar Typhimurium. *J Bacteriol* 2000;182:2245–2252.
34. Chakraborty S, Mizusaki H, Kenney LJ. A FRET-based DNA biosensor tracks OmpR-dependent acidification of *Salmonella* during macrophage infection. *Plos Biology* 2015;13.
35. Chakraborty S, Kenney LJ. A new role of OmpR in acid and osmotic stress in *Salmonella* and *E. coli*. *Front Microbiol* 2018;9.
36. Richter M, Rosselló-Móra R. Shifting the genomic gold standard for the prokaryotic species definition. *Proc Natl Acad Sci U S A* 2009;106:19126–19131.
37. Croucher NJ, Page AJ, Connor TR, Delaney AJ, Keane JA *et al*. Rapid phylogenetic analysis of large samples of recombinant bacterial whole genome sequences using Gubbins. *Nucleic Acids Res* 2015;43:e15.

38. Page AJ, Taylor B, Delaney AJ, Soares J, Seemann T *et al*. SNP-sites: rapid efficient extraction of SNPs from multi-FASTA alignments. *Microbial Genomics* 2016;2.
39. Stamatakis A. RAxML-VI-HPC: maximum likelihood-based phylogenetic analyses with thousands of taxa and mixed models. *Bioinformatics* 2006;22:2688–2690.
40. Seemann T. Prokka: rapid prokaryotic genome annotation. *Bioinformatics* 2014;30:2068–2069.
41. Page AJ, Cummins CA, Hunt M, Wong VK, Reuter S *et al*. Roary: rapid large-scale prokaryote pan genome analysis. *Bioinformatics* 2015;31:3691–3693.
42. Kurtz S, Phillippy A, Delcher AL, Smoot M, Shumway M *et al*. Versatile and open software for comparing large genomes. *Genome Biology* 2004;5.
43. Choi Y, Chan AP. PROVEAN web server: a tool to predict the functional effect of amino acid substitutions and indels. *Bioinformatics* 2015;31:2745–2747.
44. Hecht M, Bromberg Y, Rost B. Better prediction of functional effects for sequence variants. *BMC Genomics* 2015;16:S1.
45. Sim NL, Kumar P, Hu J, Henikoff S, Schneider G *et al*. SIFT web server: predicting effects of amino acid substitutions on proteins. *Nucleic Acids Res* 2012;40:W452–W7.
46. Neiger MR, Gonzalez JF, Gonzalez-Escobedo G, Kuck H, White P *et al*. Pathoadaptive alteration of *Salmonella* biofilm formation in response to the gallbladder environment. *J Bacteriol* 2019;201.
47. Park JH, Jo Y, Jang SY, Kwon H, Iriecurrency Y *et al*. The *cabABC* operon essential for biofilm and rugose colony development in *Vibrio vulnificus*. *Plos Pathog* 2015;11.
48. Datsenko KA, Wanner BL. One-step inactivation of chromosomal genes in *Escherichia coli* K-12 using PCR products. *Proc Natl Acad Sci U S A* 2000;97:6640–6645.
49. Philippe N, Alcaraz JP, Coursange E, Geiselmann J, Schneider D. Improvement of pCVD442, a suicide plasmid for gene allele exchange in bacteria. *Plasmid* 2004;51:246–255.
50. Lee ZW, Hwang SH, Choi G, Jang KK, Lee TH *et al*. A MARTX Toxin *rtxA* Gene Is Controlled by Host Environmental Signals through a CRP-Coordinated Regulatory Network in *Vibrio vulnificus*. *mBio.* 2020;11.
51. Kim SM, Lee DH, Choi SH. Evidence that the *Vibrio vulnificus* flagellar regulator FlhF is regulated by a quorum sensing master regulator SmcR. *Microbiology-Sgm* 2012;158:2017–2025.
52. Yoshida CE, Kruczkiewicz P, Laing CR, Lingohr EJ, Gannon VPJ *et al*. The *Salmonella in silico* Typing Resource (SISTR): an open web-accessible tool for rapidly typing and subtyping draft *Salmonella* genome assemblies. *PLoS One* 2016;11:1.
53. MacKenzie KD, Palmer MB, Koster WL, White AP. Examining the link between biofilm formation and the ability of pathogenic *Salmonella* strains to colonize multiple host species. *Front Vet Sci* 2017;4.
54. Desai SK, Kenney LJ. To ~P or not to ~P? non-canonical activation by two-component response regulators. *Mol Microbiol* 2017;103:203–213.
55. Desai SK, Kenney LJ. Switching lifestyles is an *in vivo* adaptive strategy of bacterial pathogens. *Front Cell Infect Microbiol* 2019;9:421.
56. Desai SK, Winardhi RS, Periasamy S, Dykas MM, Jie Y *et al*. The horizontally-acquired response regulator SsrB drives a *Salmonella* lifestyle switch by relieving biofilm silencing. *elife* 2016;5.
57. Serra DO, Richter AM, Hengge R. Cellulose as an architectural element in spatially structured *Escherichia coli* biofilms. *J Bacteriol* 2013;195:5540–5554.
58. Klumpp J, Fuchs TM. Identification of novel genes in genomic islands that contribute to *Salmonella typhimurium* replication in macrophages. *Microbiology* 2007;153:1207–1220.
59. Gal-Mor O, Gibson DL, Baluta D, Vallance BA, Finlay BB. A novel secretion pathway of *Salmonella enterica* acts as an antivirulence modulator during salmonellosis. *Plos Pathog* 2008;4.
60. Prehna G, Li Y, Stoynov N, Okon M, Vuckovic M *et al*. The zinc regulated antivirulence pathway of *Salmonella* is a multiprotein immunoglobulin adhesion system. *J Biol Chem* 2012;287:32324–32337.
61. Theoret JR, Cooper KK, Zekarias B, Roland KL, Law BF *et al*. The *Campylobacter jejuni* Dps homologue is important for in vitro biofilm formation and cecal colonization of poultry and may serve as a protective antigen for vaccination. *Clin Vaccine Immunol* 2012;19:1426–1431.
62. Prigent-Combaret C, Brombacher E, Vidal O, Ambert A, Lejeune P *et al*. Complex regulatory network controls initial adhesion and biofilm formation in *Escherichia coli* via regulation of the *csgD* gene. *J Bacteriol* 2001;183:7213–7223.
63. Gerstel U, Kolb A, Romling U. Regulatory components at the *csgD* promoter-additional roles for OmpR and integration host factor and role of the 5 ' untranslated region. *Fems Microbiol Lett* 2006;261:109–117.
64. Thomson NR, Clayton DJ, Windhorst D, Vernikos G, Davidson S *et al*. Comparative genome analysis of *Salmonella* Enteritidis PT4 and *Salmonella* Gallinarum 287/91 provides insights into evolutionary and host adaptation pathways. *Genome Res* 2008;18:1624–1637.
65. Stabler RA, He M, Dawson L, Martin M, Valiente E *et al*. Comparative genome and phenotypic analysis of *Clostridium difficile* 027 strains provides insight into the evolution of a hypervirulent bacterium. *Genome Biol* 2009;10:R102.
66. Tomomori C, Tanaka T, Dutta R, Park H, Saha SK *et al*. Solution structure of the homodimeric core domain of *Escherichia coli* histidine kinase EnvZ. *Nat Struct Biol* 1999;6:729–734.
67. Horstmann N, Saldana M, Sahasrabhojane P, Yao H, XP S *et al*. Dual-Site phosphorylation of the control of virulence regulator impacts group A streptococcal global gene expression and pathogenesis. *Plos Pathog* 2014;10.
68. Ichikawa M, Minami M, Isaka M, Tatsuno I, Hasegawa T. Analysis of two-component sensor proteins involved in the response to acid stimuli in *Streptococcus pyogenes*. *Microbiology-Sgm* 2011;157:3187–3194.
69. Flores AR, Jewell BE, Yelamanchili D, Olsen RJ, Musser JM. A single amino acid replacement in the sensor kinase LiaS contributes to a carrier phenotype in Group A *Streptococcus*. *Infect Immun* 2015;83:4237–4246.
70. Horstmann N, Tran CN, Brumlow C, DebRoy S, Yao H *et al*. Phosphatase activity of the control of virulence sensor kinase CovS is critical for the pathogenesis of group A *streptococcus*. *Plos Pathog* 2018;14.
71. White AP, Gibson DL, Grassl GA, Kay WW, Finlay BB *et al*. Aggregation via the red, dry, and rough morphotype is not a virulence adaptation in *Salmonella enterica* serovar typhimurium. *Infect Immun* 2008;76:1048–1058.
72. Tükel C, Nishimori JH, Wilson RP, Winter MG, Keestra AM *et al*. Toll-like receptors 1 and 2 cooperatively mediate immune responses to curli, a common amyloid from enterobacterial biofilms. *Cell Microbiol* 2010;12:1495–1505.
73. Pontes MH, Lee E-J, Choi J, Groisman EA. *Salmonella* promotes virulence by repressing cellulose production. *Proc Natl Acad Sci U S A* 2015;112:5183–5188.
74. Ahmad I, Lamprokostopoulou A, Le Guyon S, Streck E, Barthel M *et al*. Complex c-di-GMP signaling networks mediate transition between virulence properties and biofilm formation in *Salmonella enterica* serovar typhimurium. *PLoS One* 2011;6:e28351.
75. Winter SE, Winter MG, Godinez I, Yang HJ, Russmann H *et al*. A rapid change in virulence gene expression during the transition from the intestinal lumen into tissue promotes systemic dissemination of *Salmonella*. *Plos Pathog* 2010;6.
76. Miao EA, Leaf IA, Treuting PM, Mao DP, Dors M *et al*. Caspase-1-induced pyroptosis is an innate immune effector mechanism against intracellular bacteria. *Nat Immunol* 2010;11:1136–1142.
77. Fàbrega A, Vila J. *Salmonella enterica* serovar Typhimurium skills to succeed in the host: virulence and regulation. *Clin Microbiol Rev* 2013;26:308–341.

78. Yuk HG, Schneider KR. Adaptation of *Salmonella* spp. in juice stored under refrigerated and room temperature enhances acid resistance to simulated gastric fluid. *Food Microbiol* 2006;23:694–700.
79. Álvarez-Ordóñez A, Prieto M, Bernardo A, Hill C, López M. The acid tolerance response of *Salmonella* spp.: an adaptive strategy to survive in stressful environments prevailing in foods and the host. *Food Res Int* 2012;45:482–492.
80. Hammarlof DL, Kroger C, Owen SV, Canals R, Lacharme-Lora L *et al*. Role of a single noncoding nucleotide in the evolution of an epidemic African clade of *Salmonella*. *Proc Natl Acad Sci U S A* 2018;115:E2614–E23.
81. MacKenzie KD, Wang Y, Musicha P, Hansen EG, Palmer MB *et al*. Parallel evolution leading to impaired biofilm formation in invasive *Salmonella* strains. *PLoS Genet* 2019;15:e1008233.
82. Letunic I, Bork P. Interactive tree of life (iTOL) V3: an online tool for the display and annotation of phylogenetic and other trees. *Nucleic Acids Res* 2016;44:W242–W5.